Enhancement of Terrestrial Surface Features on High Spatial Resolution Multispectral Aerial Images

Airton Marco Polidorio
Franklin César Flores
Clélia Franco
Departamento de Informática
Universidade Estadual de Maringá
{ampolido, fcflores, cfranco}@din.uem.br
Maringá, Brasil

Nilton Nobuhiro Imai
Antonio M. G. Tommaselli
Departamento de Cartografia
Faculdade de Ciência e Tecnologia - FCT
{nnimai, tomaseli}@fct.unesp.br
Presidente Prudente, Brasil

***Abstract*—** This work introduces new transformation indexes, color and spectral-based ones, applied for features enhancement registered in aerial multispectral images acquired with high spatial resolution by the use of the newest technology in imagery airborne sensors as the digital photogrammetric cameras IGN and HRSC-AX. The new transformation indexes proposed in this work are: the *normalized Shadow Index* (*nSI*) and the *spectral Shadow Index* (*sSI*) for shadow enhancement; the *Weighted Water Index* (*WWI*) and the *Weighted Water-Soil Index* (*WWSI*) for water bodies enhancement and, the *Road Water intensity Shadow Index* (*RWSI*) for paved-road, water bodies and intensity shadowed areas enhancement.

Keywords-component; Indexes; multispectral images; image enhancement; Earth surface

I. INTRODUCTION

The first practical use of spectral response in imagery for index computing was in [1] when the *VI* (*Vegetation Index*) was applied for monitoring vegetation systems in the Great Plains. Ever since, many other indexes were proposed in order to explore the spectral response of specific features, by designing an enhanced measurement for them.

The Landsat's Thematic Mapper system has seven spectral bands, and its spectral resolution allows other transformation indexes such as *NDWI* - *Normalized Difference Water Index* - proposed by [2] and *NDVI* - *Normalized Difference Vegetation Index*. However, nowadays, most of the new photogrammetric digital cameras acquire images in four spectral bands (blue, green, red and near infrared), bringing new perspectives for photogrammetric processes automation. But due to this lower spectral resolution, only the *NDVI* is explored.

Computational imagery techniques applied to Remote Sensing and Photogrammetric Process have been used in the acquisition of previous knowledge on image-context, and significant results were achieved, such as detection or extraction of features on the ground as vegetation, water bodies, bare soil, buildings, roads and shadowed areas. This knowledge can be applied in classical computer processes, or in the design of new approaches capable of improving the results in the Photogrammetry processes. Detecting or extracting features is necessary, in many cases, to enhance them with techniques such as statistical or filtering ones. Multispectral aerial image can be enhanced by applying transformation indexes. The indexes usually provide more standardized results than those obtained by the filtering application (linear and non-linear), because these transformation indexes are less sensitive to the environment variation, mainly due to the illumination conditions during image acquisition. Besides, the indexes are not dependent on the dimension and parametric values frequently involved in the filtering processes. Moreover, most of those filters operate on intensity images only, and the transformation indexes use color and spectral attributes; for instance, *NDVI* uses reflectance values acquired in the red and infrared bands to enhance the vegetation.

This work proposes five new indexes: the *nSI* – *normalized Shadow Index*, the *sSI* – normalized *spectral Shadow*, the *WWI* – *Weighted Water Index*, the *WWSI* – *Weighted Water-Soil Index* and the *RWSI* – *Road Water intensity Shadow Index*. In order to illustrate the application of these new indexes it was proposed a set of methods for vegetation and shadowed areas segmentation, besides extracting significant markers for paved roads. All images used in this work were acquired with 20cm or 25cm of spatial resolution by the newest technology in digital photogrammetric cameras IGN (www.ign.fr) and HRSC-AX (www.dlr.de/HRSC-A), with a radiometric resolution of 8 bits.

II. INDEX COMPUTATION

Since 1960s, scientists have extracted and modeled various vegetation biophysical variables using remotely sensed data. Much of the effort has gone into the development of *vegetation indices* [3], defined as dimensionless, radiometric measures that function as indicators of relative abundance and activity of green vegetation, often including leaf-area-index, percentage green cover, chlorophyll content, green biomass, and absorbed photosynthetically active radiation. There are several

vegetation indexes in use many are summarized in [3]. Those indexes explore images acquired in several regions of the electromagnetic spectrum by use of the reflectance values R_λ computed from radiance values captured those images, where λ is a particular wavelength value, or is the center of the specific spectral band.

An index should [3]: (1) normalize or model external effects such as Sun angle; viewing angle; and the atmosphere for consistent spatial and temporal comparisons; and (2) normalize internal effects such as canopy background variations, including topography (slop and aspect) and soil variations. About *NDVI*, [4] concluded that: "Global-based operational applications of the *NDVI* have utilized digital counts, at-sensor radiances, 'normalized' reflectance (top of the atmosphere), and more recently, partially atmospheric corrected (ozone absorption and molecular scattering) reflectance. Thus, the *NDVI* has evolved with improvements in measurement inputs. Currently, a partial atmospheric correction for Rayleigh scattering and ozone absorption is used operationally for the generation of the Advanced Very High Resolution Radiometer […]. The *NDVI* is currently the only operational, global-based vegetation index utilized. This is in part, due to its 'ratioing' properties, which enable the *NDVI* to cancel out a large proportion of signal variations attributed to calibration, noise, and changing irradiance conditions that accompany changing sun angles, topography, clouds/shadow and atmospheric conditions […] the *NDVI* tends to increase for atmospherically corrected data".

Feature enhancements [5] based on indexes were developed to explore the spectral resolution of the acquired images from imagery satellites. To compute those indexes, in most cases, is necessary for the digital numbers (*DN*) of the multispectral imagery to be converted to at-satellite reflectance (*R*) to achieve radiometric consistency among images. This standard measurement unit (reflectance) allows comparison among data acquired in different dates and by different sensors.

If the sensors are onboard at a satellite-platform, the use of reflectance data to compute a certain index has accurate results, because those sensors are radiometrically calibrated and the images are acquired from different regions on Earth at the same local hour of the day and the solar angle can be accurately estimated. However, imaging activity by airborne-platform requires several hours, or days, to be finished. This delayed activity is affected by a strong alteration that occurs in the illumination conditions on the imaging area. Due to the illumination difference among images, given by the drastic alteration in the solar angle that occurs during the acquisition process, the camera operator modifies the camera configuration (e.g., *gain* and *offset*) to handle the image acquisition, in an attempt to improve the results for some photogrammetric processes (as photo interpretation). This approach hinders the computation of accurate reflectance values. Thus, in this condition, it is easier to use the *DN* values as an alternative to compute indexes like *NDVI*. This work adopts this data simplification.

III. The Proposed Indexes

This section introduces the proposed indexes. An evaluation of the results provided by these indexes is also shown. The red (*R*), green (*G*), blue (*B*) and near infrared response (*NIR*) bands are necessary to compute these indexes, as well as the intensity (*I* or *V*) and saturation (*S*) components extracted from true colors (RGB) images using the transformation RGB color system to HSI or HSV color system [6], [7], [8]. In this work, it was used the HSV color system components. The brightness values registered in the *NIR* band must be used after the accomplishment of its histogram equalization, aiming the increasing of the contrast between clear and dark features.

The first step of our process is to perform the image histogram equalization [6] to enhance only the brightness values of *NIR* band. It is important because it decreases the brightness value of very dark features and increases the brightness value of clear ones. This procedure obviously alters the near infrared spectral response behavior among the involved features. But, the basic idea of this work is to enhance features based on indexes that allow their detection from high complexity multispectral aerial images. The natural enhancement provided by the *NIR* band for vegetation, some soil type, paved-road and water bodies are increased by the histogram equalization. Several applications of histogram equalization enhancements were compared: a) to all RGB bands; b) only to *I* component; and c) to *NIR* band. All RGB bands without any enhancements were also considered. The *NIR* band histogram equalization produced the best results. All brightness values corresponding to the RGB bands, the original *NIR* image, the *NIR* image with equalized histogram and, the HSV components must be scaled to interval [0,1] for conformity of operations with the indexes values, which belongs to the interval [-1,1].

A. nSI – normalized Shadow Index

Shadows are caused by the occlusion of incident light rays by an object. The result of that occlusion produces two kinds of shadows: a) the self shadow, corresponding to the part of the object that is not directly illuminated and b) the cast shadow that corresponds to the projection of the object over other objects. The shadow is classified in two categories: *umbra* and *penumbra*. *Umbra* corresponds to the shadowed areas in which the direct light is totally blocked and, *penumbra* when the direct light is partially blocked.

For a passive imaging system, cast shadows create interferences in the scene. The effected features cannot offer the radiometric response and they cause changes on imaged features. For instance splitting features; distortion in the geometric shape of features; and, sometimes, complete loss of features. Besides these changes, the shaded areas enhance some atmospheric effects in the radiometric response onto the shaded feature. When imaging a completely shadowed area (*umbra)*, the sensor will be receiving signal from atmospheric effects that affect this area and it is not due to the absence of the radiometric response of the feature.

The main contribution to the values of the radiance registered by the sensor in umbra areas is given by the scattering component. The scattering causes a strong saturation in the shadowed areas with the electromagnetic wavelengths corresponding to the blue and violet colors. The shaded areas present low intensity due the blocked sunlight, and high saturation due to the scattering. Rayleigh demonstrated [9] that small particles in suspension in the atmosphere can cause deviations in the path of visible spectrum electromagnetic waves (blue, green and red). The quantification of that phenomenon depends on three factors: (1) the sensor height above ground; (2) the electromagnetic wavelength (λ) involved in the process; and, (3) the diameters of the particles suspended in the atmosphere.

When imaging an umbra area, the sensors in the blue and green bands should register more scattering data than the sensor of the red band. However, the perfect *umbra* does not exist in aerial imagery due to the countless secondary light sources. Another aspect is the camera configuration that can be applied. For instance, it is allowed to alter the *gain* and *offset* parameters for each band to obtain images with great variance. In other words, most of the acquired images for these cameras are not radiometric calibrated. The configurations of the cameras are set to produce a suitable image in order to ease the photo interpretation. In this image, the dark points of the scene are registered in the spectral bands with zero brightness value. These darker points usually belong to *quasi-umbra* areas and the registered brightness values should not be zero because in this case, they should register the atmospheric scattering. For intensely shadowed areas, it is expected that the sensor registers, at least, the scattering component which corresponds to the randomized change of the solar radiation path due to its interaction with small particles, gases and aerosols in suspension [10], [11].

Shadow has an unexpected behavior, which is dependent of secondary illumination sources that illuminate the shadow indirectly (multiple diffusion, neighborhood radiance and diffuse radiance effects); such behavior is also dependent on the surface brightness on which the shadow is projected. If the surface is clear, the shadows can be hard segmented or, in the worst case, confused with another dark feature. For images acquired with low spatial resolution (10m or greater), those details are not significant. However, for acquired images with high spatial resolution (1m or smaller) those details have strong influence on the radiometric shadows behavior.

A technique for shadowed areas segmentation was developed by [11]. This technique is applied to aerial color images and is based only on the color attributes of the shaded areas. Using the components *I* and *S*, from the HSI color system, the authors verified that, due to the atmospheric Rayleigh scattering, the shadows are highly saturated with the colors blue and violet and, obviously, it possesses low intensity due to the occlusion of the direct sunlight radiation. All these observations are reaffirmed by [12],[13] and they proposed an index to enhance and a method to shadows segmentation in aerial true color images using that possibility of the shadows to possess blue shades. This difference between intensity and saturation values was exploited by [11] for shadowed areas segmentation.

The *nSI* index (1) explores the values of the highest saturation *S* and the lowest intensity *V* (from HSV color system) observed from the shadow pixels to compute a normalized difference index. This index produces the highest values for dark features (as shadows and some water bodies types – Fig. 2c). The basic idea of that equation is focused on [11] observations.

$$nSI = \frac{S - V}{S + V} \tag{1}$$

B. *sSI – spectral Shadow Index*

The index s*SI* (2) follows the same reasoning of the *nSI*. The difference is that the *sSI* uses the brightness values of the *NIR* band (equalized) instead of the component *V* or *I*. The vegetation usually has a dark green color in the visible spectrum which represents a low brightness and a high saturation. In this case, the *nSI* will also produce high values for that vegetation type. The substitution of the *V* or *I* values by *NIR* values produces low *sSI* values for green vegetation. However, this new index produces higher values for water bodies due to the low brightness value registered in the *NIR* band for this feature type (Fig. 2d).

$$sSI = \frac{S - NIR}{S + NIR} \tag{2}$$

C. *WWI – Weighted Water Index*

Bare soil areas, in general, have high reflectance values in the whole region of the visible electromagnetic spectrum. Its range of spectral response is dependent on its chemical composition and humidity. In the region of the near infrared (800-1200nm) the vegetation and the dry bare soil and rocks present high reflectance values. However, for regions of the electromagnetic spectrum greater than 1400nm the differences between dry soil and vegetation are higher than other spectral bands. While the reflectance increases for dry soil, it decreases for vegetation, and it is almost zero for water (Fig. 1). The interaction of the incident luminous energy with the water is complex and it is dependent on a set of factors such as the level of diffuse reflection in the water body surface; the type and concentration of materials in suspension (for instance, chlorophyll, clay and nutrients); the type and constitution of the water body bottom and; the climatologically variables that alter the optical properties of the water bodies [14].

The brightness values of water body pixels from the equalized *NIR* band are almost zero and the respective pixels in the green (*G*) band have superior brightness values

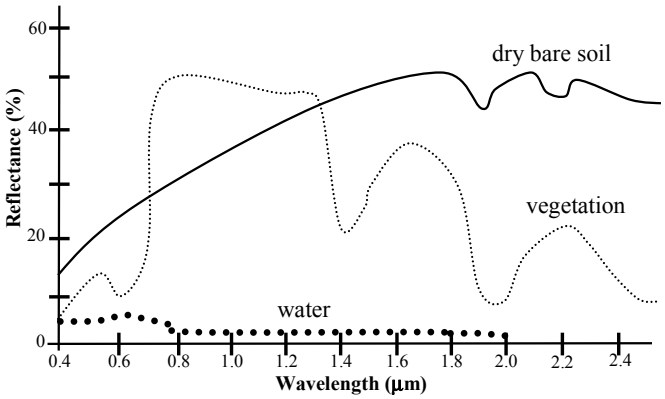

Fig. 1. Typical spectral reflectance of common Earth features: water, vegetation, and bare soil.

then, the expression $G \pm NIR \cong G$ is true. However, due to the set of factors that interfere in the optical properties of the water bodies, brightness values more significant are registered in the *NIR* band. Empiric observations allowed to establish $G \cong 4NIR$ as an equivalent relationship among those brightness values for water bodies. Therefore, it is expected that the expression $G - 4NIR$ produces values close to zero for water body pixels and negative values for features with high reflectance values in the *NIR* band (vegetation, bare soil, several types of roof buildings, etc.). The *WWI* index (eq. 3a) is applied for water body enhances (Fig. 2e).

$$WWI = \frac{G - 4NIR}{G + 4NIR} \tag{3a}$$

But the water bodies can present different colorations depending on the material in suspension. So, the equation (3a) enhances very well green water bodies. An alternative to the use of *WWI* is the *mWI* (*maximum Water Index*) (3b), which promotes a standardized enhances for water bodies, independently of its coloration. To compute the *mWI* index is necessary to use the $M = \max(R, G, B)$ values that corresponding to the maximum values registered among the RGB bands pixel-to-pixel. *M* values are equal to the values of the component *V* extracted from HSV color system. Also, is necessary to use the original brightness values registered in the *NIR* image, without histogram equalization process, due the fact of the water to absorb a lot of near infrared energy and any alteration in those values can alter the standardized enhancement promoted by the *mWI*.

$$mWI = \frac{M - NIR_{Original}}{M + NIR_{Original}} \tag{3b}$$

D. WWSI – Weighted Water-Soil Index

Equation 4 uses the same principles of equation (3a), but (4) adopts the *M* values. This change enhances the water bodies and, in different degrees, the bare soil types and the roof buildings. Another aspect promoted by this index is the cast shadow removal in the paved-road (Fig. 2f).

$$WWSI = \frac{M - 4NIR}{M + 4NIR} \tag{4}$$

E. RWSI – Road Water intensity Shadow Index

When brightness values of the band *NIR* are equalized, the contrast difference between radiant features (as vegetation and some kind of soils and roofs) and dark ones (as water bodies, paved-road and some kind of shadows) is increased. The brightness values from the intensity component (*V*) are greater than the corresponding values from the equalized *NIR* band for dark features (and smaller for bright ones). So, the *RWSI* index is computed according to (5). The enhancement for water bodies, paved-road and some kind of shadows provided by this index is very strong. Fig. 3g shows the positive values given by this index.

$$RWSI = \frac{V - NIR}{V + NIR} \tag{5}$$

IV. Indexes Results Analisis

The indexes proposed in this paper are defined in the interval [-1, 1] that could be displayed as gray level images resulting from histogram stretching processing. Equation 6 computes the histogram stretching to interval [0, 1] [7]. Fig. 2 shows the indexes results which values were stretched to the interval [0, 255] just for display purposes. The *RWSI* index is shown with only their positive values Fig. 2g.

$$f(X) = \frac{X - \min(X)}{\max(X) - \min(X)} \tag{6}$$

where, *X* is an index value to be stretched to interval [0, 1].

The behavior patterns of the proposed indexes are very stable and were observed in a set of different images. In order to show those behavior patterns, a sample set made up of 60 points from the image shown in Fig. 2a was collected based on a visual interpretation. This set of 60 points was split into six disjoint groups, each group with 10 points. The first group is on green vegetation areas. The second one is on bare soil. The third group is on building roofs. The fourth one is on paved-roads. The fifth group is on shadowed areas and the sixth one is on water bodies. Those indexes were computed for each chosen point and, the obtained result was plotted on the graphic shown in Fig. 2h. This graphic also presents the respective *NDVI* and *NIR* values for best evaluation.

An aspect that stands out in this graphic is the oscillations low-high values of *NDVI* for pixels on the shadowed areas. It is a detail that does not appear in images gotten by spatial resolution lower than 1m. Therefore, for higher spatial resolution images, it is hard to distinguish areas covered by green vegetation using only a *NDVI* thresholding since a considerable portion of shadowed areas is included as vegetation.

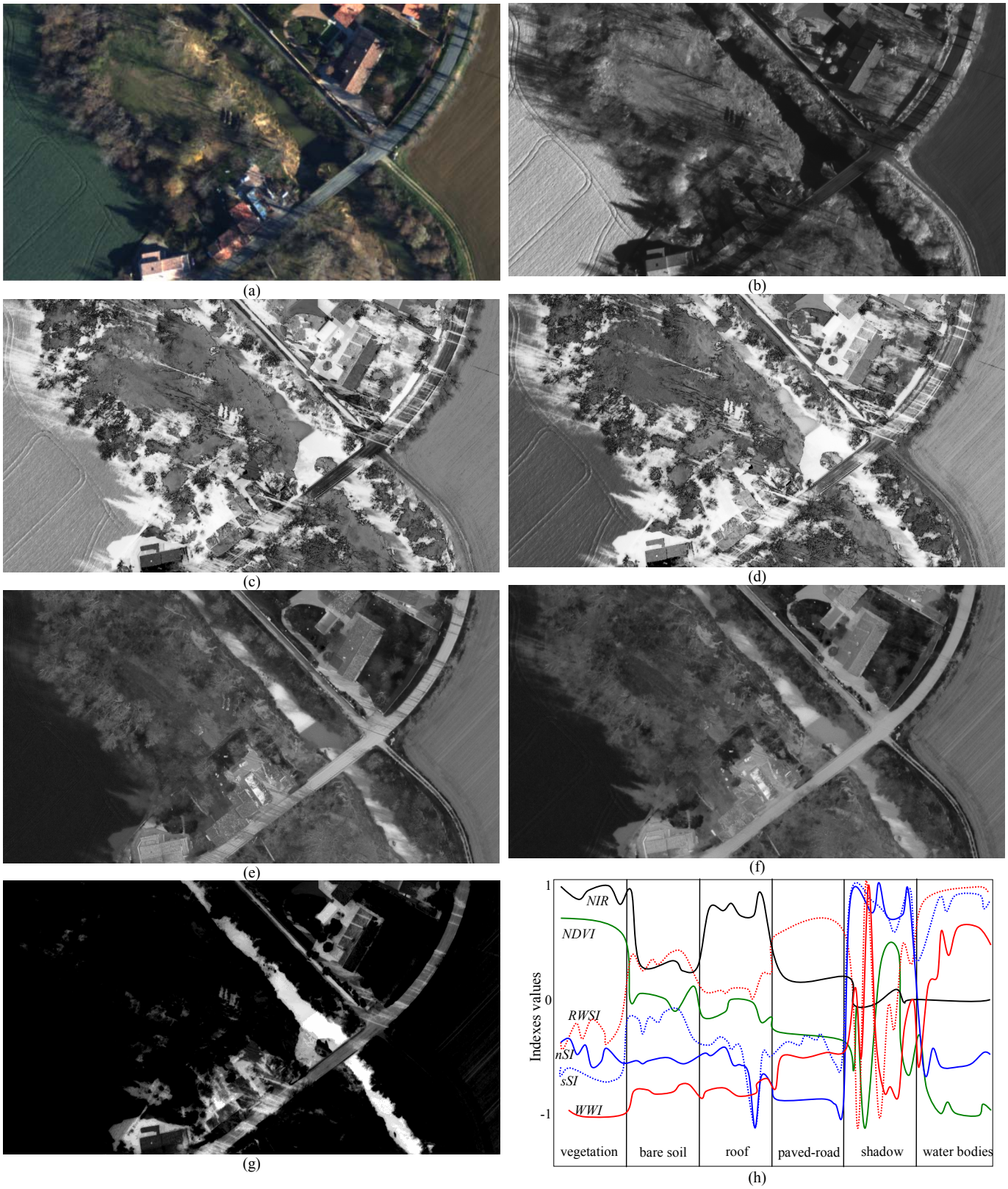

Fig. 2. Indexes results and analysis. (a) Original RGB image 25cm of spatial resolution (from IGN camera). (b) Non-equalized *NIR* band. (c) *nSI* index. (d) *sSI* index. (e) *WWI* index. (f) *WWSI* index. (g) Positive values produced from *RWSI* index. (h) Index responses to the features (green vegetation, bare soils, roof buildings, paved roads, shadowed areas and water bodies): Equalized *NIR* (black), *NDVI* (green), *nSI* (blue), *sSI* (dot-blue), *WWI* (red) and *RWSI* (dot-red).

The correlation between *WWI* and *WWSI* indexes is high mainly for the pixel values that corresponding to water bodies and paved-roads. For other features, the values produced by these indexes are smaller than –0.3, except for paved-roads. In other words, these indexes can wrongly interpret paved-roads as water bodies. The differences between *WWI* and *WWSI* are small but, for some processes a little gain can be significant. The *WWSI* index is not represented in Fig. 2h.

The *nSI* and *sSI* indexes computed the highest (and stable) values for shadowed pixels. The *sSI* also showed high values for water bodies pixels, as expected. An important characteristic presented by these indexes is the inverse correlation between vegetation and water bodies areas.

All indexes, except the *nSI* and *sSI* ones, provided very unstable values on shadowed areas. That occurs because the shadow behavior depends, among others factors, on the surface brightness where the shadow is cast and on the intensity of indirect sun light on the surface.

The *RWSI* index enhances some kinds of bare soils and shadows, but the highest and most stable values are obtained from paved-roads and water bodies.

V. CONCLUSION

The idea of applying indexes to image enhancement is not new. The key of the problem is how to develop suitable formulas for such indexes. The three bands of the visible spectrum, true RGB color images, are highly correlated and to define new indexes adopting only those bands is a very hard task and, usually, it leads to poor results. The exploitation of alternative color systems where the intensity and the color components are not associated (as HSI and HSV) is also possible. If the near infrared band is available, then new possibilities appear. This paper introduced five new indexes applied to high spatial resolution aerial imagery enhancement. These indexes are computed in function of four spectral bands that cover the visible spectrum and the near infrared range besides of two attributes extracted from HSV color system (intensity and saturation). Such indexes are used in the analysis of images acquired by cameras of low spectral resolution (4 bands) but, with high spatial resolution (GSD – Ground Sample Distance – lesser than 25cm). The indexes *nSI*, *sSI* and *WWI* were applied also in satellites imagery (Landsat and CBERS) and they produced qualitative results.

In spite the proposed methods applied to features segmentation by using the indexes introduced in this paper be very simple (using only logical and arithmetic operations), qualitative results were obtained. Despite the simplicity of the proposed applications, their results are expressive and establish the quality of the indexes applied to aerial multispectral imagery for features enhancement. The proposed indexes are significant tools, which allow the adoption of new approaches to solve or to improve the solution of many problems in Remote Sensing and Photogrammetry Sciences.

Future work includes a development of a segmentation framework where the proposed indexes are exploited to detect and segment specifics features on aerial imagery of Earth surface acquired with high spatial resolution.

ACKNOWLEDGMENT

The authors would like to thank the following institutions for providing the images used in the experiments: IGN, Institut Géographique National de France; DLR, Deutshes Zentrum für Luft-und Raumfahrt and; Digimapas and Fototerra Atividades de Aerolevantamentos.

REFERENCES

[1] J. W. Rouse, R. H. Haas, J. A. Schell and D. W. Deering, "Monitoring vegetation systems in the Great Plains with ERTS," in *Proceedings of Third Earth Resources Technology Satellite-1 Symposium*, Greenbelt: NASA SP-351, 1974, pp. 309–317.

[2] B. C. Gao, "NDWI – A normalized difference water index for remote sensing of vegetation liquid water from space," *Remote Sensing of Environment*, vol. 58, pp. 257–266, 1996.

[3] J. R. Jensen. Remote sensing of the environment: an Earth resource perspective. New Jersey: Prentice Hall, 2000.

[4] A. Huet, C. Justice, W. M. Leeuwen. *Vegetation index (MOD 13): Algorithm Theoretical Basis Document*. Version 3, 1999, 129 p. Available in: <http://modis.gsfc.nasa.gov/data/atbd/atbd_mod13.pdf>. Accessed in 2007.

[5] R. R. Irish. (2006, March). Landsat 7 science data user's handbook. National Aeronautics and Space Administration. Available in: <http://ltpwww.gsfc.nasa.gov/IAS/handbook/handbook_toc.html>.

[6] H. R. Myler and A. R. Weeks. *The Pocket Handbook of Imaging Processing Algorithms in C*. New York: Prentice-Hall Inc, 1993.

[7] R. C. Gonzalez and R. E.Woods, *Digital Image Processing*. Reading, M A: Addison-Wesley, 1992.

[8] W. K. Pratt, *Digital Image Processing*, 2nd ed. NewYork: John Wiley and Sons, 1991.

[9] Van De Hulst. *Light Scattering by Small Particles*. New York: John Wiley and Sons, 1957.

[10] T. M. Lillesand and R. W. Kiefer. *Remote Sensing and Image Interpretation*. 4th edition, New York: John Wiley & Sons Inc, 2000.

[11] A. M. Polidorio, F. C. Flores, N. N. Imai, A. M. G. Tommaselli, and C. Franco, "Automatic Shadow Segmentation in Aerial Color Images," in *IEEE Proceedings of XVI Brazilian Symposium on Computer Graphics and Image Processing*, São Carlos, Brazil, October 12-15, 2003, pp. 270–277.

[12] V. J. D. Tsai, "A comparative study on shadow compensation of color aerial images in invariant color models," IEEE Transactions on Geoscience and Remote Sensing, vol. 44, no. 6, pp. 1661—1761, June 2006.

[13] Kuo–Liang Chung, Yi–Ru Lin, and Yong–Huai Huang, *Efficient Shadow Detection of Color Aerial Images Based on Successive Thresholding Scheme*. Submitted to IEEE *Transactions on Geoscience and Remote Sensing*. Date Submitted 19-Jun-2008.

V. I. Haltrin, W. E. McBride III and R. A. Arnone, "Spectral Approach to Calculate Specular Reflection of Light from Wavy Water Surface," in *Proceedings of D. S. Rozhdestvensky Optical Society:International Conference Current Problems in Optics of Natural Waters* (ONW'2001), St. Petersburg, Russia, 2001, pp. 133-138.